

Evaluation of the Drying Stress in Industrial Kiln-dried Boards Using a Force-based Technique

Satjapan Leelatanon,^a Sataporn Jantawee,^b Sornthep Vannarat,^c and Nirundorn Matan^{a,*}

The introduction of a restoring force technique has allowed the internal stress within kiln-dried lumber to be assessed, without requiring a modulus. However, an analytical model based on the elastic beam theory was only valid within a flexural range and only internal stress in the direction of the width was assumed to exist. Within this work, the model was extended to lumber, which could also contain some other internal stress components, by testing 30-mm-thick and 100-mm- to 130-mm-wide flat-sawn rubberwood boards. The improved model successfully separated the effects of other internal stress components in terms of a remnant force. Also, a finite element analysis was employed to validate the internal stress behavior. With little impact from other internal stress components, the finite element model, which used the released strain and Young's modulus in the tangential direction, successfully simulated the restoring force profile for an entire half-split length, including the relatively short half-split length outside the flexural range. But the finite element model failed to perfectly capture the restoring force behavior in the presence of other internal stress components. Future work is required to fully investigate the internal stress in all three main orthogonal directions.

Keywords: Internal stress; Stress assessment; Restoring force technique; McMillen slice test; Finite element model

*Contact information: a: Materials Science and Engineering, School of Engineering and Resources, Walailak University, Thasala district, Nakhon Si Thammarat 80160, Thailand; b: Faculty of Industrial Technology, Nakhon Si Thammarat Rajabhat University, Meaung district, Nakhon Si Thammarat 80280, Thailand; c: Institute for Promotion of Teaching Science and Technology, 924 Sukhumvit Road, Phra Khanong, Khlong Toei, Bangkok 10110, Thailand; *Corresponding author: mnirundo@wu.ac.th*

INTRODUCTION

Internal stress is always created within a piece of lumber during kiln drying as a result of the presence of a moisture gradient, which induces differential shrinkages between the outer and inner core sections (McMillen 1958; Perré and Passard 2007). Remanufacturing of stress-containing lumber can lead to a remarkable increase in losses because of distortion (Wengert 1992; Cai and Oliveira 2004). A reliable quantitative assessment of residual stress is therefore crucial for successful quality control (Welling 1994).

Since the 1950s, several techniques have been proposed to evaluate the internal stress within lumber. The McMillen slice test (McMillen 1958) has traditionally been employed to assess the stress level by determining the mechanical response of stress relaxation within slices cut from a lumber board. The released strain in each slice can be calculated by measuring the deformation. By knowing the modulus of elasticity, the released stress in each slice can then be calculated from the measured strain (Rossini et al. 2012; Schajer and Ruud 2013). Because of difficulties in measuring the relatively small released strain of several wood slices, the prong test (Simpson 1991) and case-hardening test (ENV 14464 2010), performed by measuring the deflection caused by removing some sections or splitting the lumber instead, have commonly been employed in sawmills. In all cases, the modulus of elasticity, depending on multiple influences including species,

moisture, specific gravity, grain direction, temperature, location in a tree, *etc.* (Bodig and Jayne 1982; Matan and Kyokong 2003; Kretschmann 2010; Sonderegger *et al.* 2013; Yang *et al.* 2015; Yoshihara and Yoshinobu 2015; Hamdan *et al.* 2018), is needed to relate the measured strain or deflection profiles and internal stress.

To directly assess the magnitude of the internal stress without requiring the modulus data for the wood, a novel force-based approach for measuring the restoring force (RF) on a so-called “half-split” specimen was first proposed by Diawanich *et al.* (2012). The RF technique is suitable to assess the internal stress in materials having relatively low modulus such as wood for at least two reasons. First, the deformation related to the internal stress relaxation after cutting is relatively large so that restraining of the cut specimen back to the initial configuration is possible to perform. Second, errors related to such restraining, which are inevitable in practice, would little affect the measured RF data and therefore the derived value of the internal stress (Diawanich *et al.* 2012). For the opposite reasons, the RF technique is inappropriate to materials with high modulus such as metals and ceramics. In addition, it is not applicable to brittle materials having relatively low fracture energy in which cracks easily form (Courtney 2000).

Jantawee *et al.* (2016) later improved the measurement technique by inventing a new apparatus to secure the specimen to a steel frame while it was cut with a band saw. The net force caused by the stress relaxation was directly transferred to the connected load cell. An interpretation of the internal stress from the measured RF data was also developed by Jantawee *et al.* (2016) using the elastic beam theory. Also, a stress chart related to the measured RF has been created for convenient use in the sawmill industry. However, two important limitations still exist in the calculations used by Jantawee *et al.* (2016). First, only stress components in the direction of the width were taken into account. The effects of other stress components, including stresses in the thickness and length directions, were assumed to be negligible. Second, the analytical model that was based on the elastic cantilever beam theory was not valid outside of the flexural response range, especially at the relatively short length of the half-split in a narrow piece of lumber.

The main objective of this work was to address these two limitations. Some adjustments to the calculations were made to separate the effects of other stress components for a better estimation of the major internal stress in the direction of the width. Finite element analysis was employed to validate and gain more understanding of the internal stress behavior for an entire range of half-split lengths.

EXPERIMENTAL

Measurements of the Restoring Force and Released Strain

Fifteen pieces of flat-sawn industrial kiln-dried rubberwood lumber were taken from a local sawmill in Nakhon Si Thammarat, Thailand. The lumber was 30 mm thick (d) in the radial direction, 100 mm to 130 mm wide (W) in the tangential direction, and approximately 1 m long in the longitudinal direction. They were separated into two sets. The first set ($P_0 \sim 0$) was selected to meet the requirement set by Jantawee *et al.* (2016), which states that the internal stress mainly exists in the width direction, while other stress components are negligible. Because this kind of lumber is rare, only a single piece of lumber was used. The second set ($P_0 \neq 0$) with 15 pieces was randomly chosen. A piece of wood was removed approximately 50 mm from the end of each lumber piece before six wood specimens that were 50 mm in length were created (b) (Fig. 1a). Two adjacent specimens were used to measure the RF according to Jantawee *et al.* (2016) and measure the released strain according to the McMillen slice test (McMillen 1958). Therefore, there were three replicates for both the RF and slice test measurements for each piece of lumber.

All of the prepared specimens were free from defects. The measurements were performed at two levels of internal stress, *i.e.*, high (HS) and low internal stress (LS). Assessment of the HS was performed immediately on the day the lumber was obtained. The remaining pieces of lumber were capped with aluminum foil at both ends and were kept in a conditioning chamber at 20 °C and 65% relative humidity for four weeks. Then, the assessment of the LS was performed after the internal stress was partially relaxed.

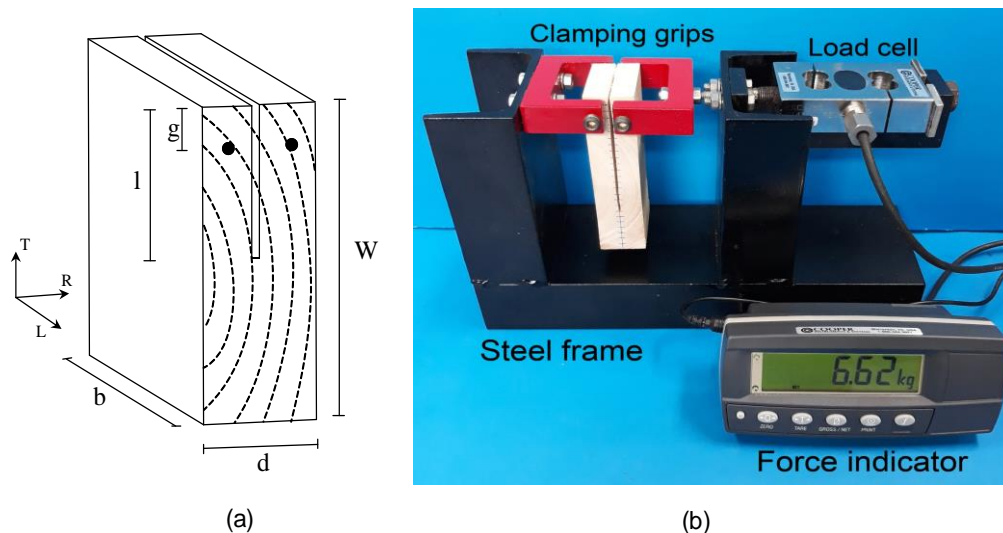


Fig. 1. (a) Diagram of the half-split specimen for the RF measurement and (b) a half-split specimen installed in the RF measuring device

The RF measurement was performed using the device (In-House Made, Walailak University, Nakhon Si Thammarat, Thailand) that is shown in Fig. 1b. The specimen was clamped to the steel frame with screws at a distance (g) of 10 mm from the top surface. A small amount of torque, ranging from 2 N·m to 3 N·m, was applied to hold the specimen in place with a contact screw area of 24 mm² without damaging the wood tissue (Jantawee *et al.* 2016). While clamped to the frame, the specimen was cut at half thickness in the width direction along the half-split length (l , mm). The RF was recorded at 5-mm intervals. For the McMillen slice test, the specimen surfaces were first slightly planed in the thickness direction to remove irregularities and obtain a relatively smooth surface before being marked by dividing lines, so that it could be cut into six equal slices. The initial width of each pre-marked slice (W_b , mm) was measured by calipers with a precision of 0.01 mm. The specimens were then cut into slices along the dividing lines. Each slice was subsequently pressed flat before its width (W_a , mm) was measured. The released strain (ε , mm/mm) of each slice was calculated according to Eq. 1:

$$\varepsilon = \frac{W_a - W_b}{W_b} \quad (1)$$

All of the slices were tested to determine the Young's modulus in the tangential direction (E_T) using a universal testing machine (150kN, Lloyd Instruments, UK) equipped with a strain gauge (Epsilon Technology, USA). A section of each slice was also weighed before and after oven-drying at 103 °C ± 2 °C for 24 h to determine its moisture content.

Finite Element Analysis of the Restoring Force Technique

To validate the mechanical response of the clamped half-split specimen, a three-dimensional finite element (FE) model was generated using SOLID186 elements in the software ANSYS (v12, Ansys Inc., Pennsylvania, USA). The tetrahedral SOLID186 used in this study is a three-dimensional 10-node solid element having three degrees of freedom

at each node. It is well suited for modeling the residual stress in solid materials. The computation accuracy is high enough for this study because SOLID186 exhibits quadratic displacement behavior. Also, the results obtained from ten-node tetrahedrons are much better than those from simple four-node models (Zhan *et al.* 2015; Kloiber *et al.* 2017). The constitutive model of linear elasticity for three mutually orthogonal materials was given in the computational process. According to Bodig and Jayne (1982), all of the moduli were determined as ratios of the measured modulus of elasticity in the tangential direction ($E_L:E_R:E_T = 20:1.6:1$; $G_{LR}:G_{LT}:G_{RT} = 10:9.4:1$; and $E_L:G_{LR} = 14:1$). Three Poisson's ratios were estimated to be 0.02 (μ_{RL}), 0.02 (μ_{LT}), and 0.35 (μ_{RT}) (Bodig and Jayne 1982; Kretschmann 2010). Because the specimen had two planes of symmetry, only a quarter of the specimen (Fig. 2) was constructed to reduce the computational time in the solving process. Two planes of symmetry, LT and RT, were fixed in the R- and L-directions, respectively. All elements were fixed the edge length to not larger than 2.0 mm, so number of elements was automatically generated from the specified edge length. By using this size of element, the system was well able to allow the outputs to reach convergence. Also, satisfactory accuracy was achieved in a suitable computation time. All of the nodes in the clamping (screw) area were restrained in the R-direction to deduce the calculated RF. The released strain and Young's modulus data of the $P_0=0$ and $P_0\neq 0$ lumber sets that were determined by the McMillan slice test were applied to the layers that corresponded to the tests.

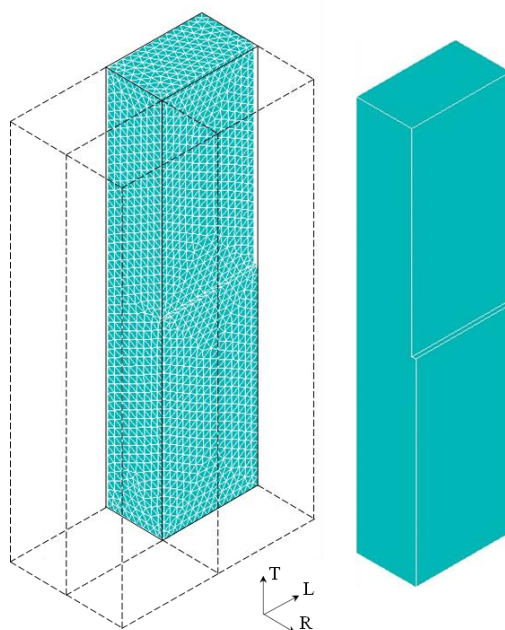


Fig. 2. The 3D mesh for a quarter of the wood specimen used in finite element simulation

RESULTS AND DISCUSSION

Analytical Calculation of the Internal Stress in the Presence of Other Stress Components

For a piece of lumber that was half-split at a particular length (l , mm), the value of the RF P (N) is proportional to the maximum internal stress in the width direction (σ_m , MPa), which was assumed to linearly vary from the outer surface through the inner core, according to Eqs. 2 and 3,

$$P = \frac{4bl^2}{Sd} \sigma_m \quad (2)$$

$$S = \frac{32(l-g)^2(2l+g)}{d^3} \quad (3)$$

where S is the geometrical factor (Jantawee *et al.* 2016).

The variable P has been shown to be proportional to the term $4bl^2/Sd$ with a zero intercept at a relatively low $4bl^2/Sd$ value or at a relatively long half-split length in the so-called flexural response range. Consequently, the magnitude of σ_m in the width direction can be directly obtained from the slope of the graph plotted of P and $4bl^2/Sd$. The effect of other stress components was neglected in the above calculation, and all of the lumber boards examined by Jantawee *et al.* (2016) were selected to contain a relatively low level of stress in the other directions. This was the case for the $P_o \sim 0$ set of specimens (Fig. 3a) which was a rare case, and just only one lumber out of fifteen lumbars was found in this study. The magnitudes of σ_m derived from the graphs were 2.62 MPa for the HS specimens and 1.02 MPa for the LS specimens.

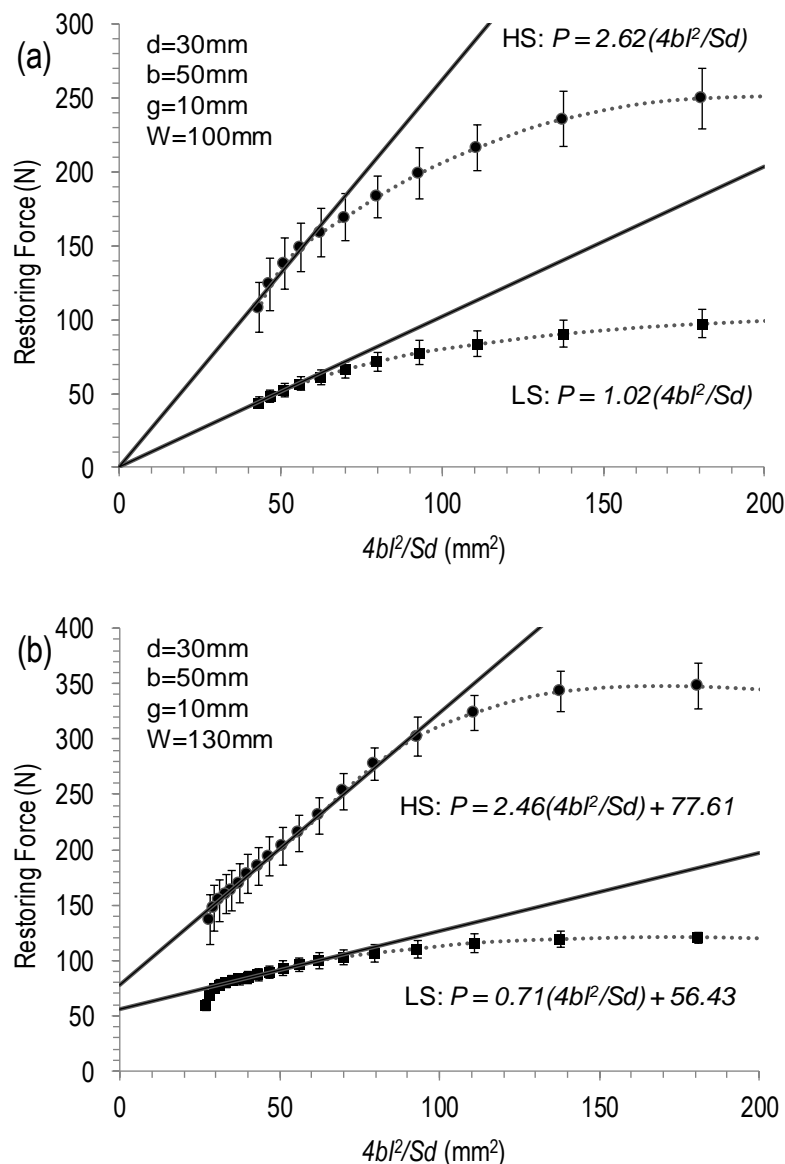


Fig. 3. Plots of the RF versus $4bl^2/Sd$ for the 30-mm-thick half-split (a) $P_o \sim 0$ and (b) $P_o \neq 0$ rubberwood specimens, which contained relatively high and low levels of internal stress; solid lines represent the best fits to the experimental data in the flexural response range

The above limitation was removed in this work. All fourteen flat-sawn boards ($P_o \neq 0$) were randomly selected without any restrictions. They all had the same typical trend when P was plotted against $4bl^2/Sd$ shown in Fig. 3b. The linear relationship between P and $4bl^2/Sd$ was still observed in the flexural response range, but with a positive value for the y-intercept. Therefore, Eq. 2 was modified to Eq. 4,

$$P = \frac{4bl^2}{Sd} \sigma_m + P_o \quad (4)$$

where P_o , the y-intercept, is the remnant RF value (N) when the term $4bl^2/Sd$ is equal to zero.

The RF remains when the half-split length approaches infinity. The magnitudes of σ_m and P_o derived from the graphs were 2.46 MPa and 77.61 N for the HS specimens and 0.71 MPa and 56.42 N for the LS specimens, respectively (Fig. 3b). During conditioning of the specimens at 20 °C and a 65% relative humidity, the σ_m was reduced by 71% from 2.46 MPa to 0.71 MPa, while the P_o was reduced by 27% from 77.61 N to 56.42 N.

The plots of P against $4bl^2/Sd$ for the other randomly selected lumber boards (15 boards) also showed similar behaviors and were governed by Eq. 4 (data not shown). Therefore, Eq. 4 must universally apply to any piece of lumber. The first term in Eq. 4 is the RF caused by the flexural response of the internal stress relaxation in the width (tangential) direction after half-splitting, as mentioned by Jantawee *et al.* (2016). The presence of P_o was expected to have been caused by the relaxation of other stress components, especially in the thickness and length directions, which were irrelevant to bending of the legs of the half-specimen. A further investigation into the possible origin of P_o using the FE model was performed in this study.

Finite Element Analysis of the Restoring Force of the Lumber Containing the Main Internal Stress

The FE model was first employed to describe the RF profiles of the HS and LS specimens that were prepared from the $P_o \sim 0$ lumber set, similar to those reported by Jantawee *et al.* (2016), in which the internal stress in the width (tangential) direction mainly exists in the lumber. The effects of other stress components, including stresses in the thickness (radial) and length (longitudinal) directions, on the RF were assumed to be negligible. The released strain and Young's modulus data across the specimen thickness prior to half-splitting were obtained by the McMillan slice test of the $P_o \sim 0$ set of the kiln-dried rubberwood lumber at two levels of internal stress (HS and LS). These data are listed in Table 1, and the values were used as the initial inputs for the FE model. As was expected for the case-hardened kiln-dried lumber, the negative and positive released strain values observed in the inner and outer sections of the lumber after slicing, respectively, were caused by the tensile and compressive stresses remaining within the inner and outer sections, respectively (McMillen 1958). The magnitudes of the Young's modulus across the thickness of all of the specimens examined were roughly uniform. The values were within the standard deviation. However, the Young's modulus in the HS specimens was higher than that in the LS specimens because of the lower moisture content prior to conditioning of the HS specimens (Jiang *et al.* 2014; Babiak *et al.* 2018).

Finite Element Analysis of the Restoring Force of the Lumber Containing Other Stress Components

Using the released strain and Young's modulus data in the width (tangential) direction for the $P_o \neq 0$ set of specimens (Table 1), the simulated FE profiles and measured RF profiles of the HS and LS specimens are plotted in Fig. 5. Although the magnitude of the simulated RF was at the same level as the measured one on average, the RF profiles as

a function of the half-split length were clearly inconsistent. The difference manifested itself in the LS specimens, which contained a relatively low level of internal stress, especially with a relatively long half split length (Fig. 5). It was assumed in the FE model that the relaxed stress components, obtained from the McMillen slice test, were only in the width (tangential) direction. As a result, the FE-simulated RF profile roughly conformed to the pattern of P_o equal to 0, which was similar to the patterns in Fig. 4. This indicated that the relaxation of some other internal stress components that should exist within the lumber were not accounted for in the FE model. Additionally, the amount of released strain measured using the McMillen slice test, used as inputs in the FE model, should have been affected by the internal stress relaxation in other orthogonal directions (Bodig and Jayne 1982), especially the thickness direction. This result is rather complex and requires a full investigation into the internal stress relaxation in all three main orthogonal directions (tangential, radial, and longitudinal), which will be a subject of future work.

Table 1. Released Strain, Young's Modulus, and Moisture Content Data in the Tangential Direction of the $P_o \sim 0$ and $P_o \neq 0$ Sets of the Kiln-dried Rubberwood Lumber

Type of Lumber	Input	Stress Level	Distance from the Center in the Thickness Direction (mm)		
			2.5	7.5	12.5
$P_o \sim 0$	Released Strain (ϵ , %)	HS	-0.19 (0.03)	-0.06 (0.03)	+0.28 (0.06)
		LS	-0.10 (0.02)	-0.01 (0.03)	+0.12 (0.02)
	Young's Modulus (E_T , MPa)	HS	543 (64)	555 (49)	588 (54)
		LS	467 (48)	487 (54)	427 (51)
	Moisture Content (%)	HS	6.2 (0.4)	5.9 (0.4)	5.4 (0.4)
		LS	10.7 (0.2)	10.9 (0.2)	11.4 (0.3)
$P_o \neq 0$	Released Strain (ϵ , %)	HS	-0.15 (0.05)	0.03 (0.07)	+0.50 (0.12)
		LS	-0.16 (0.05)	-0.07 (0.03)	+0.11 (0.08)
	Young's Modulus (E_T , MPa)	HS	808 (19)	825 (20)	847 (20)
		LS	633 (23)	622 (26)	594 (23)
	Moisture Content (%)	HS	5.6 (0.2)	5.5 (0.1)	5.0 (0.3)
		LS	10.2 (0.4)	11.5 (0.7)	13.1 (0.5)

Note: numbers in parentheses are the standard deviation.

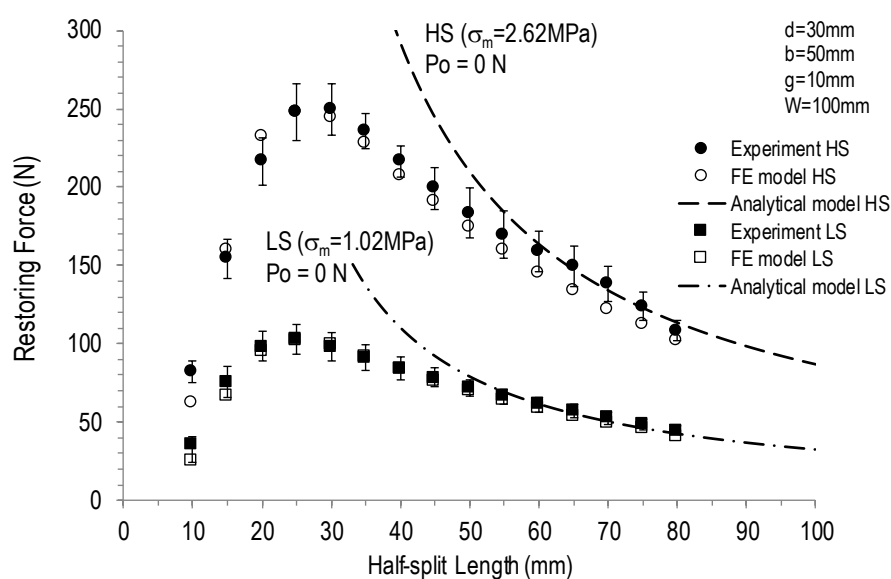


Fig. 4. Comparison of the experimental (filled symbols) and FE simulated RF (open symbols) profiles of the 30-mm-thick $P_o \sim 0$ half-split HS and LS specimens as a function of the half-split length; profiles of the calculated RF based on an elastic cantilever beam theory (solid lines) with $P_o = 0$ were also plotted for comparison

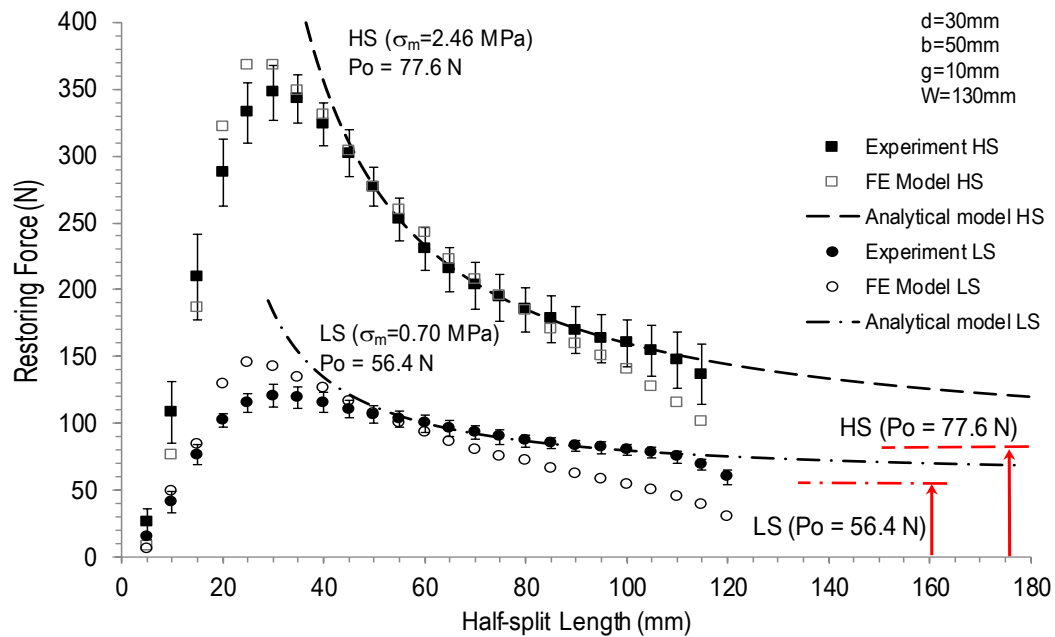


Fig. 5. Comparison of the experimental (filled symbols) and FE simulated RF (open symbols) profiles of the 30-mm-thick $P_o \neq 0$ half-split HS and LS specimens as a function of the half-split length; profiles of the calculated RF based on an elastic cantilever beam theory (solid lines) with $P_o \neq 0$ were also plotted for comparison

CONCLUSIONS

1. A general form of an analytical model based on the elastic cantilever beam theory was successfully developed to directly quantify the main internal drying stress in the width direction of kiln-dried lumber. The lumber could also contain other stress components. The RF measured on a half-split specimen was separated into two independent terms, namely a flexural force caused by the relaxation of the main internal drying stress and a force caused by the relaxation of other stress components.
2. With little effect from other internal stress components, by using the released strain and Young's modulus data in the width (tangential) direction obtained from the McMillen slice test, a numerical model based on FE analysis successfully simulated the RF profile for an entire range of half-split lengths. This included the RF profile at a relatively short half-split length, where the model based on the elastic cantilever beam theory failed.
3. In the presence of other stress components, the released strain and Young's modulus data in the width (tangential) direction were insufficient to describe the RF behavior for the entire half-split length. The FE model must be improved to incorporate some missing stress components.

ACKNOWLEDGMENTS

The authors gratefully acknowledge the Thailand Research Fund and Walailak University for their financial support (Grant No. RSA5880025) and the National e-Science Infrastructure Consortium for providing computing resources that have partly contributed to the research results reported in this paper. Special thanks go to Nakornsri Parawood Co., Ltd. of Nakhon Si Thammarat for providing the kiln-dried rubberwood lumber used within this work.

REFERENCES CITED

- Babiak, M., Gaff, M., Sikora, A., and Hysek, Š. (2018). "Modulus of elasticity in three- and four-point bending of wood," *Compos. Struct.* 204, 454-465. DOI: 10.1016/j.compstruct.2018.07.113
- Bodig, J., and Jayne, B. A. (1982). *Mechanics of Wood and Wood Composites*, Van Nostrand Reinhold Company, New York, NY.
- Cai, L., and Oliveira, L. C. (2004). "Equalizing and conditioning spruce-pine-subalpine fir lumber," *Forest Prod. J.* 54, 126-131.
- Cortney, T., H. (2000). *Mechanical Behavior of Materials*, second Ed. McGraw-Hill, New York, NY.
- Diawanich, P., Tomad, S., Matan, N., and Kyokong, B. (2012). "Novel assessment of casehardening in kiln-dried lumber," *Wood Sci. Technol.* 46(1-3), 101-114. DOI: 10.1007/s00226-010-0384-9
- ENV 14464 (2010). "Sawn timber. Method for assessment of case-hardening," European Committee for Standardization, Stockholm, Sweden.
- Hamdan, S., Rahman, Md. R., Jusoh, I., and Wahid, H. A. (2018). "Dynamic Young's modulus and moisture content of tropical wood species across sap, median, and internal wood regions," *BioResources* 13(2), 2907-2915. DOI: 10.15376/biores.13.2.2907-2915
- Jantawee, S., Leelatanon, S., Diawanich, P., and Matan, N. (2016). "A new assessment of internal stress within kiln-dried lumber using a restoring force technique on a half-split specimen," *Wood Sci. Technol.* 50(6), 1277-1292. DOI: 10.1007/s00226-016-0852-y
- Jiang, J. H., Lu, J. X., Zhou, Y. D., Zhao, Y. K., and Zhao, L. Y. (2014). "Compression strength and modulus of elasticity parallel to grain of oak wood at ultra-low and high temperatures," *BioResources* 9(2), 3571-3579. DOI: 10.15376/biores.9.2.3571-3579
- Kloiber, M., Kunecký, J., Drdácáký, M., Tippner, J., and Sebera, V. (2017). "Experimental and numerical analysis of semi-destructive device for in situ assessment of wood properties in compressive parallel to grain," *Wood Sci. Technol.* 51(2), 345-356. DOI: 10.1007/s00226-016-0881-6
- Kretschmann, D. E. (2010). "Mechanical properties of wood," in: *Wood Handbook (Wood as an Engineering Material)*, R. J. Ross (ed.), U.S. Department of Agriculture Forest Service Forest Products Laboratory, Madison, WI, pp. 5.1-5.46.
- Matan, N., and Kyokong, B. (2003). "Effect of moisture content on some physical and mechanical properties of juvenile rubberwood (*Hevea brasiliensis* Muell. Arg)," *Songklanakarin Journal of Science and Technology* 25(3), 327-340.
- McMillen, J. M. (1958). *Stresses in Wood During Drying* (Report No. 1652), U.S. Department of Agriculture Forest Products Laboratory, Madison, WI.
- Perré, P., and Passard, J. (2007). "Stress development," in: *Fundamentals of Wood Drying*, P. Perré (ed.), European COST A.R.BO.LOR., Nancy, France, pp. 243-271.
- Rossini, N. S., Dassisti, M., Benyounis, K. Y., and Olabi, A. G. (2012). "Methods of measuring residual stresses in components," *Mater Design* 35, 572-588.
- Schajer, G. S., and Ruud, C. O. (2013). "Overview of residual stresses and their measurement," in: *Practical Residual Stress Measurement Methods*, G. S. Schajer (ed.) John Wiley & Sons, West Sussex, pp. 1-27.
- Simpson, W. T. (1991). *Dry Kiln Operator's Manual* (Agriculture Handbook AH-188), Forest Products Laboratory, U.S. Department of Agriculture Forest Products Laboratory, Madison, WI.
- Sonderegger, W., Martienssen, A., Nitsche, C., Ozyhar, T., Kaliske, M., and Niemz, P. (2013). "Investigations on the physical and mechanical behavior of sycamore maple

- (*Acer pseudoplatanus* L.),” *Eur. J. Wood Wood Prod.* 71(1), 91-99. DOI: 10.1007/s00107-012-0641-8
- Welling, J. (1994). *EDG-Recommendation: Assessment of Drying Quality of Timber*, European Drying Group (EDG), Hamburg, Germany.
- Wengert, E. (1992). *Techniques for Equalizing and Conditioning Lumber* (No. 65), University of Wisconsin, Madison, WI.
- Yang, B. Z., Seale, R. D., Shmulsky, R., Dahlen, J., and Wang, X. (2015). “Comparison of nondestructive testing methods for evaluating no. 2 southern pine lumber: Part A, Modulus of elasticity,” *Wood and Fiber Science* 47(4), 375-384.
- Yoshihara, H., and Yoshinobu, M. (2015). “Young’s modulus and shear modulus of solid wood measured by the flexural vibration test of specimens with large height/length ratios,” *Holzforchung* 69(4), 493-499. DOI: 10.1515/hf-2014-0151
- Zhan, J., Fard, M., and Jazar, R. (2015). “A quasi-static FEM for estimating gear load capacity,” *Measurement* 75, 40-49.

Article submitted: December 5, 2018; Peer review completed: March 2, 2019; Revised version received: April 10, 2019; Accepted: April 11, 2019; Published: April 17, 2019. DOI: 10.15376/biores.14.2.4403-4412